Monograph:
Tokhi, M.O. and Hossain, M.A. (1994) Adaptive Active Control of Noise and Vibration. Research Report. ACSE Research Report 534 . Department of Automatic Control and Systems Engineering

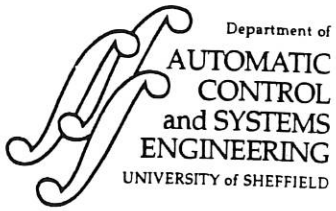

ADAPTIVE ACTIVE CONTROL OF NOISE AND VIBRATION

M O Tokhi and M A Hossain

Department of Automatic Control and Systems Engineering, The University of Sheffield,
P O Box 600, Mappin Street, Sheffield, S1 4DU, UK.

Tel: (0742) 825136.
Fax: (0742) 731 729.
E-mail: O.Tokhi@sheffield.ac.uk.

Research Report No. 534

August 1994

Abstract

The design and implementation of an active control mechanism for noise cancellation and vibration suppression within an adaptive control framework is presented. A control mechanism is designed within a feedforward control structure on the basis of optimum cancellation at an observation point. The design relations are formulated such that to allow on-line design and implementation and thus result in a self-tuning control algorithm. The algorithm is implemented on an integrated digital signal processing and transputer system and results verifying the performance of the algorithm are presented and discussed.

Key words: *Active noise control, active vibration control, self-tuning control.*

CONTENTS

1 Introduction

Noise and vibration have long been recognised as sources of environmental pollution, having adverse effects on human life in numerous ways. Many attempts have been made in the past at devising methods of tackling the problems arising from unwanted noise and vibration. Traditional methods of noise cancellation and vibration suppression utilise passive control techniques which consist of mounting layers of passive materials on or around the source. Investigations have shown that these methods are efficient at high frequencies but expensive and bulky at low frequencies (Leitch and Tokhi, 1987; Tokhi and Leitch, 1991a).

Active noise/vibration control consists of artificially generating cancelling source(s) to destructively interfere with the unwanted source and thus result in a reduction in the level of the noise/vibration (disturbances) at desired location(s). This is realised by detecting and processing the noise/vibration by a suitable electronic controller so that when superimposed on the disturbances cancellation occurs. Due to the broadband nature of these disturbances, it is required that the control mechanism realises suitable frequency-dependent characteristics so that cancellation over a broad range of frequencies is achieved. In practice, the spectral contents of these disturbances as well as the characteristics of system components are in general subject to variation, giving rise to time-varying phenomena. This implies that the control mechanism is further required to be intelligent enough to track these variations, so that the desired level of performance is achieved and maintained.

In many practical applications the problem of noise and vibration are found to be closely related. For example, a close coherence is observed in numerous situations between the two due to secondary effects (Tokhi and Leitch, 1991b). In these cases a control solution aimed at reducing, for example the level of vibration will result in significant reduction in the level of noise and, to some extent, vice versa (Snyder and Hansen, 1991). The control of noise and vibration by active means is based on the same design principle.

This has been utilised here in the development of an active control strategy for both noise cancellation and vibration suppression.

Active noise/vibration control is not a new concept. It is based on the principles that were initially proposed by Lueg in the early 1930s for noise cancellation (Lueg, 1936). Since then a considerable amount of research work has been devoted to the development of methodologies for the design and realisation of active noise/vibration control systems in various applications (Baz and Poh, 1988; Baz and Ro; 1991; Baz et.al, 1990a,b; Burton, 1993; Clark and Fuller, 1991; Doelman, 1991; Firoozian and Stanway, 1988; Fuller et.al, 1992; Jayasuriya and Chopra, 1990; Kourmoulis, 1990; Krishnamurthy and Chao, 1992; Leitch and Tokhi, 1987; Lu et.al, 1989; Lueg, 1936; Snyder and Hansen, 1991, 1992; Tanaka and Kikushima, 1988; Tokhi and Leitch, 1991a,b; Tzou and Gadre, 1990; Yaniv and Horowitz, 1990). Not much work has been done in investigating the problems of noise and vibration together (Doelman, 1991). Thus, it will be advantageous to consider tackling the two problems within a unified design strategy.

This paper presents an investigation into the development of an active control mechanism for noise cancellation and vibration suppression within an adaptive control framework. An active noise control (ANC) system is designed on the basis of optimum cancellation of broadband noise at an observation point in a linear three-dimensional propagation medium. The controller design relations are formulated such that to allow on-line design and implementation and, thus, yield a self-tuning control algorithm. The algorithm is implemented on an integrated digital signal processing (DSP) -transputer system and its performance assessed within a simulated three-dimensional free-field medium.

A flexible beam system in transverse vibration is considered in fixed-free and fixed-fixed forms for vibration suppression. Such a system has an infinite number of resonance modes although in most cases the lower modes are the dominant ones requiring attention. First order central finite difference (FD) methods are used to study the behaviour of the beam and develop a suitable test and verification platform. The unwanted vibrations in the structure are assumed to be caused by a single point disturbance of broadband nature.

These are detected and suitable suppression signals generated via a point actuator to yield vibration suppression over a broad frequency range along the beam. The self-tuning control algorithm developed within the ANC system is implemented on the integrated DSP-transputer system and its performance assessed.

2 Active noise control

A schematic diagram of the geometrical arrangement of a feedforward ANC structure is shown in Figure 1. An unwanted (primary) point source emits broadband noise into the propagation medium. This is detected by a detector located at a distance r_e relative to the primary source, processed by a controller of suitable transfer characteristics and fed to a cancelling (secondary) point source located at a distance d relative to the primary source and a distance r_f relative to the detector. The secondary signal thus generated is superimposed on the primary signal so that to achieve cancellation of the noise at and in the vicinity of an observation point located at distances r_g and r_h relative to the primary and secondary sources respectively.

A frequency-domain equivalent block diagram of the ANC structure is shown in Figure 1(b), where E, F, G and H are transfer functions of the acoustic paths through the distances r_e, r_f, r_g and r_h respectively. M, M_o, C and L are transfer characteristics of the detector, the observer, the controller and the secondary source respectively. U_D and U_C are the primary and secondary signals at the source locations whereas Y_{OD} and Y_{OC} are the corresponding signals at the observation point respectively. U_M is the detected signal and Y_O is the observed signal. The block diagram in Figure 1(b) can be thought of either in the continuous frequency (s) domain or the discrete frequency (z) domain. Therefore, unless specified, the analysis and design developed in this paper apply to both the continuous-time and the discrete-time domains.

The detected and observed signals, namely U_M and Y_O in Figure 1(b), can each be thought of as composed of sum of two signals one due to the primary source and one due to the secondary source. Using the block diagram in Figure 1(b), these can be expressed as

$$\begin{aligned} U_M &= MEU_D + MFU_C \\ Y_O &= M_O GU_D + M_O HU_C \end{aligned} \tag{1}$$

The secondary source signal U_C, on the other hand, can be expressed, through the controller path as,

$$U_C = CLU_M \tag{2}$$

For complete cancellation of the noise to be achieved at the observation point the condition

$$Y_O = 0 \tag{3}$$

must be satisfied. This is equivalent to the minimum variance design criterion in a stochastic environment. This requires the primary and secondary signals at the observation point to be equal in amplitudes and have a phase difference of 180^0 relative to each other. Thus, synthesising the controller within the block diagram of Figure 1(b) on the basis of this objective yields

$$C = \frac{G}{ML(FG - EH)} \tag{4}$$

Equation (4) is the required controller transfer function for optimum cancellation of broadband noise at the observation point. In designing the controller, causality is ensured by making the number of zeros in C either less than or equal to the number of its poles.

Note in equation (4) that, for given secondary source and detector the controller characteristics are determined by the geometric arrangement of system components. This incorporates the location of the detector and the observer with respect to the primary and

secondary sources. Among these, there exist arrangements that will lead to the denominator, $FG - EH$, in equation (2) approaching zero and thus requiring the controller to have impractically large gain. Thus, an analysis of the system on this basis yielding the locus of detection and observation points for which the controller will be required to have an impractically large gain for optimum cancellation is important at a design stage.[3] Moreover, note in Figure 1(b) that the secondary signals reaching the detector form a positive feedback loop that can cause the system to become unstable for certain geometrical arrangements of system components. Therefore, an analysis of the system from a stability point of view leading to a robust design of the system is important at a design stage (Tokhi and Leitch, 1991c).

2.1 Self-tuning active noise control

In practice, the characteristics of sources of noise vary due to operating conditions leading to time-varying spectra. Moreover, the characteristics of transducers, sensors and other electronic equipment used are subject to variation due to environmental effects, ageing, etc. To design an ANC system so that the controller characteristics are updated in accordance with these changes in the system such that the required performance is achieved and maintained, a self-tuning control strategy, allowing on-line design and implementation of the controller, can be utilised.

Self-tuning control is distinguished as a class of adaptive control mechanisms (Harris and Billings, 1981; Tokhi and Leitch, 1992; Wellstead and Zarrop, 1991). It essentially consists of the processes of identification and control, both implemented on-line. The identification process is mainly concerned with on-line modelling of the plant to be controlled and, thus, incorporates a suitable system identification algorithm. The control process, on the other hand, is concerned with the design and implementation of the controller using the plant model and, thus, incorporates a suitable controller design criterion. In this manner, various types of self-tuning control algorithms can be designed depending on the type of the identification algorithm and controller design strategy

employed. Many system identification schemes have been used in self-tuning control algorithms. Among these, the recursive form of the least squares algorithm which produces unbiased estimates of a plant model (in parametric form), based on measurements of the input and output signals of the plant, has proved to be the most useful and practically successful self-tuning identifier (Tokhi and Leitch, 1992). In a similar manner, several controller design criteria have been used in self-tuning control algorithms. Among these, the most common ones are the minimum variance and pole assignment designs.[26] A self-tuning control algorithm can either be designed as an explicit combination of identification of a plant model and controller design or as an implicit algorithm in which the controller is identified directly (bypassing identification of the plant model). Each of these algorithms have their advantages and disadvantages which depend mainly on the application and availability of resources for implementation. Self-tuning is, in a sense, the simplest possible adaptive control algorithm derivable from the point of view of the discrete-time stochastic control theory. An attractive property of the self-tuning controller is that under most reasonable circumstances, as the number of input and output samples tends to infinity, it will converge to the optimal controller that would be obtained if the system parameters are exactly known. Moreover, the strategy is simple enough to allow the use of digital processors for implementing self-tuning controllers, thus promising a relatively low cost solution to complex control problems. In this paper an explicit self-tuning ANC algorithm, incorporating a recursive least squares (RLS) parameter estimation algorithm and the minimum variance design criterion, is developed.

Consider the system in Figure 1 as a single-input single-output (SISO) system with the detected signal, U_M, as input and the observed signal, Y_O, as output. Moreover, owing to the state of the secondary source let the system behaviour be characterised by two sub-systems, namely, when the secondary source is *off*, with an equivalent transfer function denoted by Q_0, and when the secondary source is *on*, with an equivalent transfer function denoted by Q_1. Using the block diagram of Figure 1(b), these can be obtained as

$$Q_0 = \frac{M_o G}{ME} \quad , \quad Q_1 = \frac{M_o G}{ME}\left[1 - \frac{ML(FG - EH)}{G}\right] \tag{5}$$

Note that in obtaining Q_0 and Q_1 in equation (5) the controller block in Figure 1 is replaced simply by a switch; prior to an estimation/measurement process the controller transfer function is not known. Manipulating equation (5) and using equation (4) yields an equivalent design relation for the controller in terms of Q_0 and Q_1 as

$$C = \left[1 - \frac{Q_1}{Q_0}\right]^{-1} \tag{6}$$

Equation (6) is the required controller design rule given in terms of transfer characteristics Q_0 and Q_1 which can be measured/estimated on-line. An on-line design and implementation of the controller can thus be achieved by *(a)* obtaining Q_0 and Q_1 using a suitable system identification algorithm (e.g. an RLS parameter estimation algorithm), *(b)* using equation (6) to calculate the controller transfer function and *(c)* implementing the controller on a digital processor. Moreover, to monitor system performance and update the controller characteristics upon changes in the system a supervisory level control can be utilised. This results in a self-tuning ANC mechanism as depicted in Figure 2. The 'plant' in Figure 2 designates the system in Figure 1 between the detection and observation points, in which during the identification process the controller is replaced by a switch. During the control process, however, the estimated controller transfer function is implemented to replace the switch. The supervisor is designed to monitor system performance on the basis of a pre-specified quantitative measure of cancellation as an index of performance, so that if the cancellation achieved is within the specified range then the algorithm implementation remains at the control level. However, if the cancellation is outside the specified range then self-tuning is re-initiated at the identification level.

In implementing the self-tuning control algorithm described above, several issues of practical importance need to be given careful consideration. These include properties of the disturbance signal, robustness of the estimation and control, system stability and

and the frequency of the wave. Thus, for known distances the frequency response of the acoustic paths in Figure 1(a) can be obtained. These can then be utilised within the block diagram in Figure 1(b) to calculate signal propagation through the system. A fast Fourier transform (FFT) algorithm is utilised to transform the signals concerned from time-domain into frequency-domain and vice versa as required.

The self-tuning ANC algorithm was implemented on an integrated DSP-transputer system incorporating an i860 DSP device and a T805 transputer using DSP and parallel processing (PP) methods to allow efficient and relatively accurate implementation. The DSP device with its extensive signal processing power is a 64 bit processor and is capable of 80 MFLOPs. The transputer, on the other hand, with its powerful communication facility, is a 32 bit processor capable of 4 MFLOPs. The operational configuration of this system is shown in Figure 3. This comprises of an IBM compatible PC, A/D and D/A conversion facility, a TTM110 board incorporating the transputer and the DSP device. The ANSI C toolset is used as common software for program development and implementation.

To assess the performance of the algorithm a broadband (0-512 Hz) PRBS signal was used as the unwanted primary noise. Figure 4(a) shows the autopower spectral density of the noise at the observation point before cancellation as $G_{D_o}(\omega)$ and after cancellation as $G_{oo}(\omega)$. Figure 4(b) shows the difference $G_{D_o}(\omega) - G_{oo}(\omega)$, i.e. the actual attenuation in the spectral density of the noise. It is noted that an average broadband cancellation level of 20-25 dB below 150 Hz and more than 40 dB cancellation above 150 Hz is achieved. As compared with previous implementations using DSP devices only this significant level of cancellation over a broad range of frequencies is due to the computing power achieved by the utilisation of DSP and PP methods.

3 Active vibration control

Active vibration control (AVC) is realised in a similar manner as ANC. The design of an AVC system depends upon the complexity of the structure under consideration and the nature of the disturbance process. A flexible beam system is considered in transverse vibration in fixed-free and fixed-fixed forms. Such a system has an infinite number of resonance modes although in most cases the lower modes are the dominant ones requiring attention. A schematic diagram of the AVC system, incorporating a fixed-free beam, is shown in Figure 5. The unwanted vibrations in the structure are assumed to be caused by a single point disturbance force (U_D) of broadband nature. These are detected by a point detector, processed by a controller to generate suitable suppression signals (U_C) via a point actuator so that to yield vibration suppression over a broad frequency range at an observation point along the beam. A frequency-domain equivalent block diagram of the AVC system in Figure 5 will give rise to that of the ANC system in Figure 1(b), with a similar interpretation of the transfer functions and signals involved. In this manner, the required controller transfer function for optimum vibration suppression at the observation point is, therefore, given as in equation (4) with the corresponding equivalent relation suitable for on-line design and implementation as in equation (6). Therefore, a similar formulation of the self-tuning control algorithm developed for noise cancellation applies to vibration suppression in Figure 5, yielding a self-tuning AVC algorithm.

3.1 Simulation algorithm

A schematic diagram of the cantilever beam system is shown in Figure 6, where L represents the length of the beam, $U(x,t)$ represents an applied force at a distance x from the fixed (clamped) end of the beam at time t and $y(x,t)$ is the deflection of the beam from its stationary (unmoved) position at the point where the force has been applied. The motion of the beam in transverse vibration is governed by the well known fourth-order partial differential equation (PDE) (Virk and Kourmoulis, 1988)

$$\mu^2 \frac{\partial^4 y(x,t)}{\partial x^4} + \frac{\partial^2 y(x,t)}{\partial t^2} = \frac{1}{m} U(x,t) \tag{7}$$

where μ is a beam constant given by $\mu^2 = \frac{EI}{\rho A}$, with ρ, A, I and E representing the mass density, cross-sectional area, moment of inertia of the beam and the Young's modulus respectively, and m is the mass of the beam. The corresponding boundary conditions at the fixed and free ends of the beam are given by

$$\begin{aligned} y(0,t) = 0 \quad &\text{and} \quad \frac{\partial y(0,t)}{\partial x} = 0 \\ \frac{\partial^2 y(L,t)}{\partial x^2} = 0 \quad &\text{and} \quad \frac{\partial^3 y(L,t)}{\partial x^3} = 0 \end{aligned} \tag{8}$$

To construct a suitable platform for test and verification of the AVC mechanism, a method of obtaining numerical solution of the PDE in equation (7) is required. The finite element (FE) method has commonly been used in the past for obtaining numerical solutions of the PDE and for constructing simulation environments characterising the behaviour of such systems (Chen and Ku, 1990; Lin and Trethewey, 1990; Tzou and Tseng, 1990; Udupa and Varadan, 1990). This method allows irregularities in the structure and mixed boundary conditions to be handled. However, these are not of concern in the case of a uniform beam structure considered here. Moreover, the computational effort and consequent software coding involved in the FE method makes it unfavourable for uniform structures. It has been reported that the FD method is more suitable in the simulation of uniform beam structures and simpler than the FE method (Kourmoulis, 1990). Therefore, the FD method is used here thus obtaining a numerical solution of the PDE in equation (7) and for constructing a suitable simulation environment characterising the behaviour of the beam.

To obtain a solution to the PDE, describing the beam motion, the partial derivative terms $\frac{\partial^4 y(x,t)}{\partial x^4}$ and $\frac{\partial^2 y(x,t)}{\partial x^2}$ in equation (7) and the boundary conditions in equation (8)

are approximated using first order central FD approximations. This involves a discretisation of the beam into a finite number of equal-length sections (segments), each of length Δx, and considering the beam motion (deflection) for the end of each section at equally-spaced time steps of duration Δt. In this manner, let $y(x,t)$ be denoted by $y_{i,j}$ representing the beam deflection at point i at time step j (grid-point i,j). Let $y(x+v\Delta x, t+w\Delta t)$ be denoted by $y_{i+v,j+w}$, where v and w are non-negative integer numbers.

Using a first-order central FD method the partial derivatives $\frac{\partial^2 y}{\partial t^2}$ and $\frac{\partial^4 y}{\partial x^4}$ can be approximated as

$$\frac{\partial^2 y(x,t)}{\partial t^2} = \frac{y_{i,j+1} - 2y_{i,j} + y_{i,j-1}}{(\Delta t)^2}$$
$$\frac{\partial^4 y(x,t)}{\partial x^4} = \frac{y_{i+2,j} - 4y_{i+1,j} + 6y_{i,j} - 4y_{i-1,j} + y_{i-2,j}}{(\Delta x)^4} \qquad (9)$$

Substituting for $\frac{\partial^2 y}{\partial t^2}$ and $\frac{\partial^4 y}{\partial x^4}$ from equation (9) into equation (7) and simplifying yields

$$y_{i,j+1} = 2y_{i,j} - y_{i,j-1} - \lambda^2\{y_{i+2,j} - 4y_{i+1,j} + 6y_{i,j} - 4y_{i-1,j} + y_{i-2,j}\} + \frac{(\Delta t)^2}{m}U(x,t) \qquad (10)$$

where, $\lambda^2 = \frac{(\Delta t)^2}{(\Delta x)^4}\mu^2$. Equation (10) gives the deflection of point i along the beam at time step $j+1$ in terms of the deflections of the point at time steps j and $j-1$ and deflections of points $i-1$, $i-2$, $i+1$ and $i+2$ at time step j. Note that in evaluating the deflection at the grid point $i=1$ the fictitious deflection $y_{-1,j}$ will be required. Similarly, in evaluating the deflection at the free end of the beam, $i=n$ (n representing the total number of sections along the beam), the fictitious deflections $y_{n+1,j}$ and $y_{n+2,j}$ will be required. To obtain these, the boundary conditions in equation (8) are used. In a similar manner as

above, the boundary conditions in equation (8) can be expressed in terms of the FD approximations as

$$\begin{aligned} y_{0,j} &= 0 \quad , \quad \frac{y_{1,j} - y_{-1,j}}{2\Delta x} = 0 \\ \frac{y_{n+1,j} - 2y_{n,j} + y_{n-1,j}}{(\Delta x)^2} &= 0 \quad , \quad \frac{y_{n+2,j} - 2y_{n+1,j} + 2y_{n-1,j} - y_{n-2,j}}{2(\Delta x)^3} = 0 \end{aligned} \tag{11}$$

Solving equation (11) for the deflections $y_{-1,j}$ and $y_{0,j}$ at the fixed end and $y_{n+1,j}$ and $y_{n+2,j}$ at the free end yields

$$\begin{aligned} y_{0,j} &= 0 \quad \text{and} \quad y_{-1,j} = y_{1,j} \\ y_{n+1,j} &= 2y_{n,j} - y_{n-1,j} \quad \text{and} \quad y_{n+2,j} = 2y_{n+1,j} - 2y_{n-1,j} + y_{n-2,j} \end{aligned} \tag{12}$$

Equations (10) and (12) give the complete set of relations necessary for the construction of the simulation algorithm. Substituting the discretised boundary conditions for the fixed and free ends from equations (12) into equation (10) yield the beam deflection at the grid points along the beam as

$$\begin{aligned} y_{1,j+1} &= -y_{1,j-1} - \lambda^2\{(7 - \frac{2}{\lambda^2})y_{1,j} - 4y_{2,j} + y_{3,j}\} + \phi \\ y_{2,j+1} &= -y_{2,j-1} - \lambda^2\{-4y_{1,j} + (6 - \frac{2}{\lambda^2})y_{2,j} - 4y_{3,j} + y_{4,j}\} + \phi \\ &\vdots \\ y_{n,j+1} &= -y_{n,j-1} - \lambda^2\{2y_{n-2,j} + -4y_{n-1,j} + (2 - \frac{2}{\lambda^2})y_{n,j}\} + \phi \end{aligned}$$

where, $\phi = \dfrac{(\Delta t)^2}{m} U(x,t)$. The above equations can be written in a matrix form as

$$Y_{j+1} = -Y_{j-1} - \lambda^2 S Y_j + (\Delta t)^2 U(x,t)\frac{1}{m} \tag{13}$$

where,

$$Y_{j+1} = \begin{bmatrix} y_{1,j+1} \\ y_{2,j+1} \\ \vdots \\ y_{n,j+1} \end{bmatrix}, \quad Y_j = \begin{bmatrix} y_{1,j} \\ y_{2,j} \\ \vdots \\ y_{n,j} \end{bmatrix}, \quad Y_{j-1} = \begin{bmatrix} y_{1,j-1} \\ y_{2,j-1} \\ \vdots \\ y_{n,j-1} \end{bmatrix},$$

and S is a stiffness matrix, given (for $n = 20$, say) as

$$S = \begin{bmatrix} a & -4 & 1 & 0 & 0 & 0 & \cdots & \cdots & 0 \\ -4 & b & -4 & 1 & 0 & 0 & \cdots & \cdots & 0 \\ 1 & -4 & b & -4 & 1 & 0 & \cdots & \cdots & 0 \\ 0 & 1 & -4 & b & -4 & 1 & \cdots & \cdots & 0 \\ \cdots & \cdots & \cdots & \cdots & \cdots & \cdots & \cdots & \cdots & \cdots \\ \cdots & \cdots & \cdots & \cdots & \cdots & \cdots & \cdots & \cdots & \cdots \\ \cdots & \cdots & \cdots & \cdots & 1 & -4 & b & -4 & 1 \\ \cdots & \cdots & \cdots & \cdots & 0 & 1 & -4 & c & -2 \\ \cdots & \cdots & \cdots & \cdots & 0 & 0 & 2 & -4 & d \end{bmatrix}$$

where, $a = 7 - \frac{2}{\lambda^2}$, $b = 6 - \frac{2}{\lambda^2}$, $c = 5 - \frac{2}{\lambda^2}$ and $d = 2 - \frac{2}{\lambda^2}$. Equation (13) is the required relation for the simulation algorithm, characterising the behaviour of the flexible beam system, which can be implemented on a digital computer easily.

Considering the beam in fixed-fixed form the corresponding discretised boundary conditions to equation (10) are given by

$$\begin{aligned} y_{0,j} = 0 \quad , \quad & \frac{y_{1,j} - y_{-1,j}}{2\Delta x} = 0 \\ y_{n,j} = 0 \quad , \quad & \frac{y_{n-1,j} - y_{n+1,j}}{2\Delta x} = 0 \end{aligned} \tag{14}$$

Thus, discretisation of the PDE with the boundary conditions for this case can be carried out in a similar manner as for the fixed-free beam. This will result the same relation given

in equation (13) with the stiffness matrix, for example with the beam divided into n-2 equal length segments (n grid points), for n=21 say, as

$$S \approx \begin{bmatrix} a & -4 & 1 & 0 & 0 & 0 & \cdots & \cdots & 0 \\ -4 & b & -4 & 1 & 0 & 0 & \cdots & \cdots & 0 \\ 1 & -4 & b & -4 & 1 & 0 & \cdots & \cdots & 0 \\ 0 & 1 & -4 & b & -4 & 1 & \cdots & \cdots & 0 \\ \cdots & \cdots & \cdots & \cdots & \cdots & \cdots & \cdots & \cdots & \cdots \\ \cdots & \cdots & \cdots & \cdots & \cdots & \cdots & \cdots & \cdots & \cdots \\ \cdots & \cdots & \cdots & \cdots & 1 & -4 & b & -4 & 1 \\ \cdots & \cdots & \cdots & \cdots & 0 & 1 & -4 & b & -4 \\ \cdots & \cdots & \cdots & \cdots & 0 & 0 & 1 & -4 & a \end{bmatrix}$$

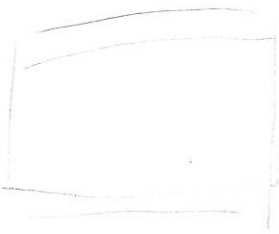

3.2 *Implementation and results*

Investigations were carried out to determine a suitable number of segments the beam under consideration be divided into so that reasonable accuracy is achieved by the simulation algorithm. This was, thus, chosen as 19 and 20 sections for the fixed-free and the fixed-fixed forms respectively. To investigate the performance of the self-tuning AVC algorithm in broadband vibration suppression the beam simulation algorithm, as a test and evaluation platform was implemented on the integrated DSP-transputer system. The investigations here were focused onto a broad frequency range covering almost all the resonance modes of the beam. To assess the performance of the algorithm a fixed (finite-duration) disturbance was used as the unwanted primary disturbance (U_D).

3.2.1 Fixed-free beam

The self-tuning algorithm for the beam in fixed-free form was realised with the primary and secondary sources located at grid points 15 and 19 respectively, the detector at grid-point 15 and the observer at grid-point 11 along the beam. Figure 7(a) shows the performance of the self-tuning control algorithm, where $G_{Do}(\omega)$ and $G_{oo}(\omega)$ represent the autopower

spectral densities of the vibration signal at the observation point before and after cancellation respectively. Figure 7(b) shows the difference $G_{Do}(\omega)-G_{oo}(\omega)$, i.e. the attenuation in the spectral density. It is noted that an average cancellation level of more than 25 dB is achieved over the full broad frequency range of the disturbance. The sharp spikes/dips noted in Figure 7(b) correspond to the resonance modes of vibration of the beam. The corresponding time domain descriptions of the beam fluctuation before and after cancellation are shown in Figure 8. It is noted that the level of unwanted disturbance is significantly reduced throughout the length of the beam. This is further evidenced in the corresponding frequency-domain description in Figure 9 given in terms of the average signal power throughout the length of the beam.

3.2.2 Fixed-fixed beam

The self-tuning algorithm for the beam in fixed-fixed form was realised with the primary and secondary sources located at grid points 10 and 9 respectively, the detector at grid-point 10 and the observer at grid-point 8 along the beam. Figure 10(a) shows the performance of the algorithm, where $G_{Do}(\omega)$ and $G_{oo}(\omega)$ represent the autopower spectral densities of the vibration signal at the observation point before and after cancellation respectively. Figure 10(b) shows the attenuation in the spectral density. It is noted that an average cancellation level of more than 25 dB is achieved over the full broad frequency range of the disturbance. The corresponding time- domain descriptions of the beam fluctuation before and after cancellation are shown in Figure 11. It is noted that the level of unwanted disturbance is significantly reduced throughout the length of the beam. This is further evidenced in the corresponding frequency-domain description in Figure 12 given in terms of the average signal power throughout the length of the beam.

4 Conclusion

The design and implementation of a self-tuning control algorithm for ANC and AVC have been presented, discussed and verified through simulation experiments. An active control mechanism for broadband cancellation of noise and vibration has been developed within an adaptive control framework. The algorithm, thus developed and implemented on an integrated DSP-transputer system, incorporates on-line design and implementation of the controller in real-time. Moreover, a supervisory level control has been incorporated within the control mechanism which allows on-line monitoring of system performance and controller adaptation. The performance of the algorithm has been verified in the cancellation of broadband noise in a free-field medium and in the suppression of broadband vibration in flexible beam structures of fixed-free and fixed-fixed forms. A significant amount of cancellation has been achieved over the full frequency range of the disturbance in each case. These demonstrate the significance of the self-tuning control mechanism for broadband noise cancellation and vibration suppression.

5 Acknowledgements

Mr Hossain is supported by a research fellowship of the Association of Commonwealth Universities.

6 References

BAZ, A. and POH, S. (1988). "Performance of an active control system with piezoelectric actuators", Journal of Sound and Vibration, **126**, (2), pp. 327-343.

BAZ, A. and RO, J. (1991). "Active control of flow-induced vibrations of a flexible cylinder using direct velocity feedback", Journal of Sound and Vibration, **146**, (1), pp. 33-45.

BAZ, A., GILHEANY, J. and STEIMEJ, P. (1990a). "Active vibration control of propeller shafts", Journal of Sound and Vibration, **136**, (3), pp. 361-372.

BAZ, A., IMAM, K. and McCOY, J. (1990b). "Active vibration control of flexible beams using shape memory actuators", Journal of Sound and Vibration, **140**, (3), pp. 437-456.

BURTON, A. W. (1993). "Active vibration control in automotive chassis systems", IEE Computing and Control Engineering Journal, **4**, (5), pp. 225-232.

CHEN, L.-W. and KU, D.-M. (1990). "Dynamic stability analysis of a rotating shaft by finite element method", Journal of Sound and Vibration, **143**, (1), pp. 143-151.

CLARK, R. L. and FULLER, C. R. (1991). "Control of sound radiation with adaptive structures", Journal of Intelligent Systems and structures, **2**, pp. 431-452.

DOELMAN, N. J. (1991). "A unified control strategy for the active reduction of sound and vibration", Journal of Intelligent Material Systems and Structure, **2**, pp. 558-580.

FIROOZIAN, R. and STANWAY, R. (1988). "Active vibration control of turbomachinery: A numerical investigation of modal controllers", Mechanical Systems and Signal Processing, **2**, (3), pp. 243-264.

FULLER, C. R., ROGERS, C. A. and ROBERTSAW, H. H. (1992). "Control of sound radiation with active/adaptive structures", Journal of Sound and Vibration, **157**, (1), pp. 19-39.

HARRIS, C. J. and BILLINGS, S. A. (1981). "Self-tuning and adaptive control: Theory and applications", Peter Peregrinus, London.

JAYASURIYA, S. and CHOPRA, S. (1990). "Active quenching of set of predetermined vibratory modes of a beam by a single fixed point actuator", International Journal of Control, **51**, (2), pp. 445-467.

KOURMOULIS, P. K. (1990). "Parallel processing in the simulation and control of flexible beam structure system", PhD. Thesis, Department of Automatic Control and Systems Engineering, The University of Sheffield, UK.

KRISHNAMURTHY, K. and CHAO, M.-C. (1992). "Active vibration control during deployment of space structures", Journal of Sound and Vibration, **152**, (2), pp. 205-218.

LEITCH, R. R. and TOKHI, M. O. (1987). "Active noise control systems", IEE Proceedings-A, **134**, (6), pp. 525-546.

LIN, Y.-H. and TRETHEWEY, M. W. (1990). "Finite element analysis of elastic beams subjected to moving dynamic loads", Journal of Sound and Vibration, **136**, (2), pp. 323-342.

LU, J., CROCKER, M. J. and RAJU, P. K. (1989). "Active vibration control using wave control concepts", Journal of Sound and Vibration, **134**, (2), pp. 364-368.

LUEG, P. (1936). "Process of silencing sound oscillations", US Patent No. 2 043 416.

SNYDER, S. D. and HANSEN, C. H. (1991). "Mechanism of active noise control by vibration sources", Journal of Sound and Vibration, **147**, (3), pp. 519-525.

SNYDER, S. D. and HANSEN, C. H. (1992). "Design consideration for active noise control systems implementing the multiple input, multiple output LMS algorithm", Journal of Sound and Vibration, **159**, (1), pp. 157-174.

TANAKA, N. and KIKUSHIMA, Y. (1988). "Rigid support active vibration isolation", Journal of Sound and Vibration, **125**, (3), pp. 539-553.

TOKHI, M. O. and LEITCH, R. R. (1991a). "Design and implementation of self-tuning active noise control systems", IEE Proceedings-D, **138**, (4), pp. 421-430.

TOKHI, M. O. and LEITCH, R. R. (1991b). "Design of active noise control systems operating in three-dimensional dispersive propagation medium", Noise Control Engineering Journal, **36**, (1), pp. 41-53.

TOKHI, M. O. and LEITCH, R. R. (1991c). "The robust design of active noise control systems based on relative stability measures", Journal of the Acoustical Society of America, **90**, (1), pp. 334-345.

TOKHI, M. O. and LEITCH, R. R. (1992). "Active noise control", Clarendon Press, Oxford.

TZOU, H. S. and GADRE, M. (1990). "Active vibration isolation and excitation by piezoelectric slab with constant feedback gains", Journal of Sound and Vibration, **136**, (3), pp. 477-490.

TZOU, H. S. and TSENG, C. I. (1990). "Distributed piezoelectric sensor/actuator design for dynamic measurement/control of distributed parameter systems: A piezoelectric finite element approach", Journal of Sound and Vibration, **138**, (1), pp. 17-34.

UDUPA, K. M. and VARADAN, T. K. (1990). "Hierarchical finite element method for rotating beams", Journal of Sound and Vibration, **138**, (3), pp. 447-456.

VIRK, G. S. and KOURMOULIS, P. K. (1988). "On the simulation of systems governed partial differential equations", Proceedings of Control-88, Conference, pp. 318-321.

WELLSTEAD, P. E. and ZARROP, M. B. (1991). "Self-tuning systems - Control and signal processing", John Wiley, Chichester.

YANIV, O. and HOROWITZ, I. (1990). "Quantitative feedback theory for active vibration control synthesis", International Journal of Control, **51**, (6), pp. 1251-1258.

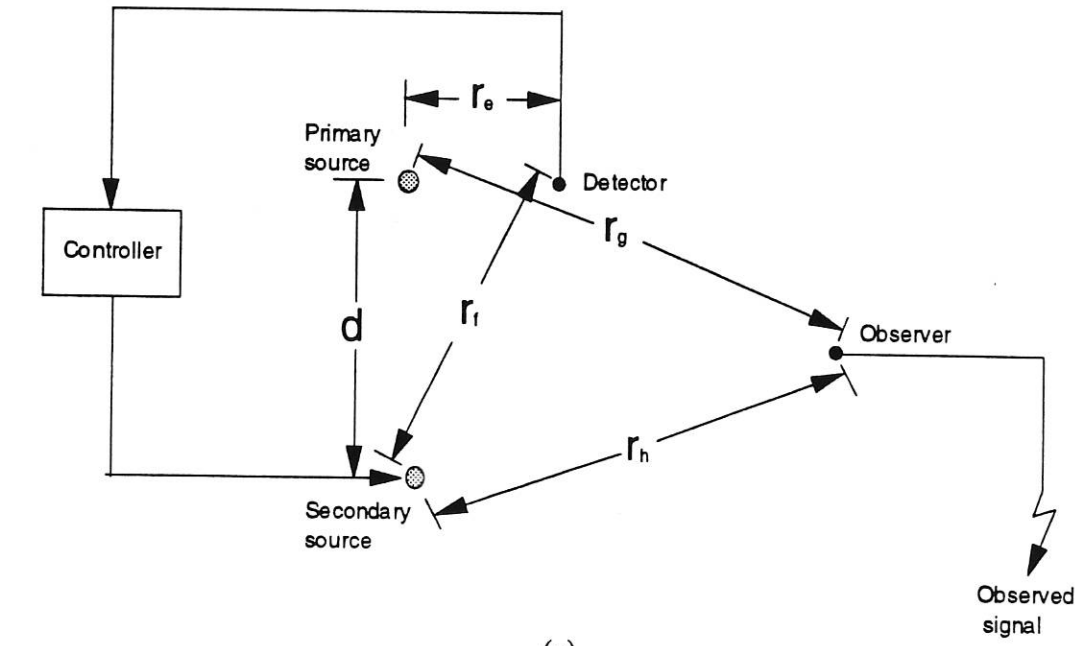

(a)

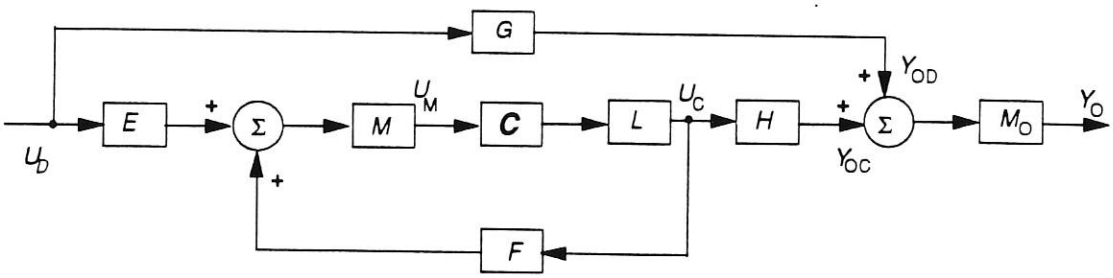

(b)

Figure 1: Active noise control structure;
(a) Schematic diagram.
(b) Block diagram.

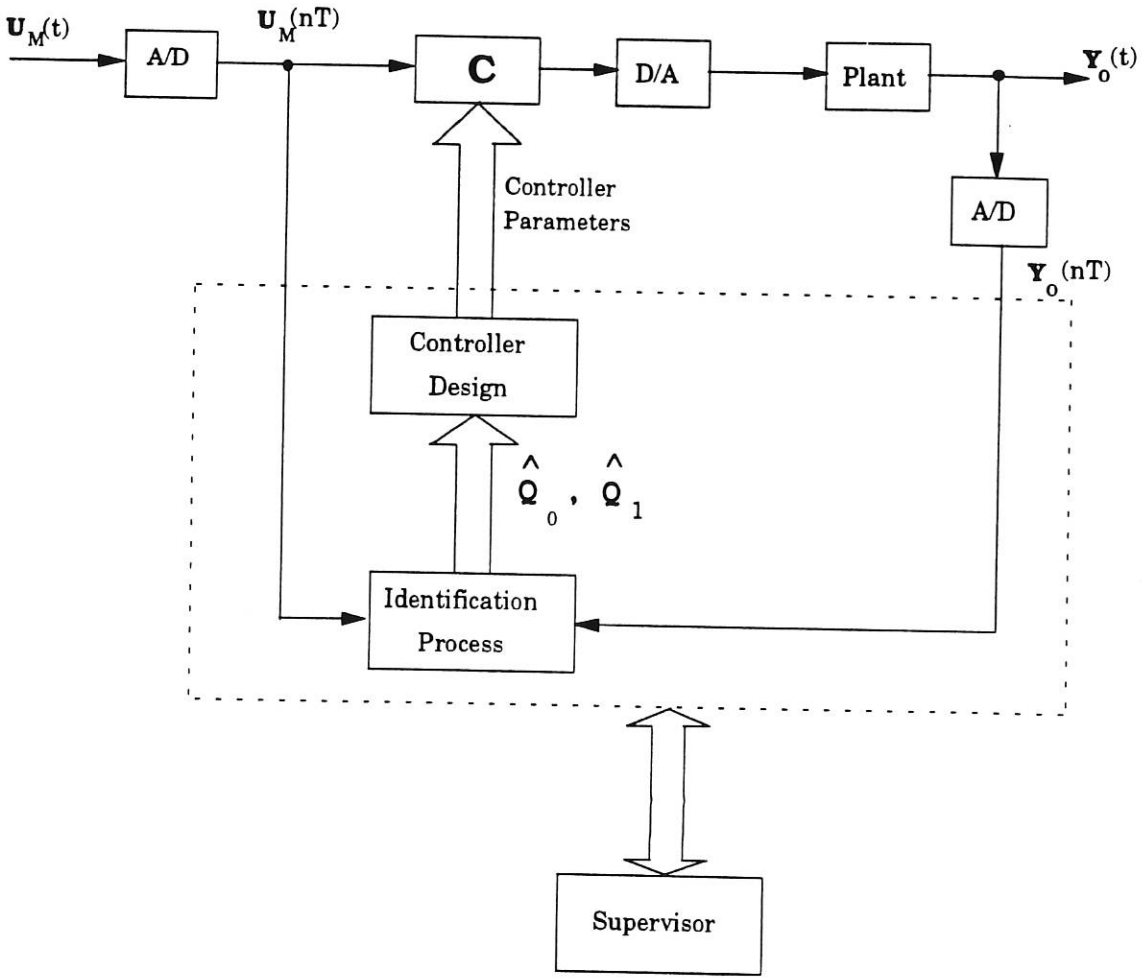

Figure 2: Self-tuning controller

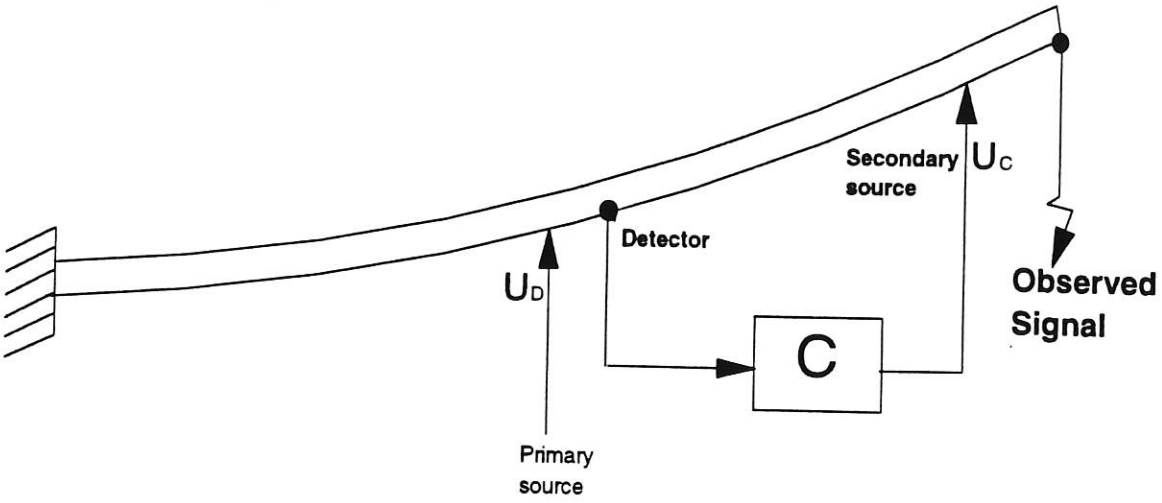

Figure 5: Schematic diagram of the AVC structure

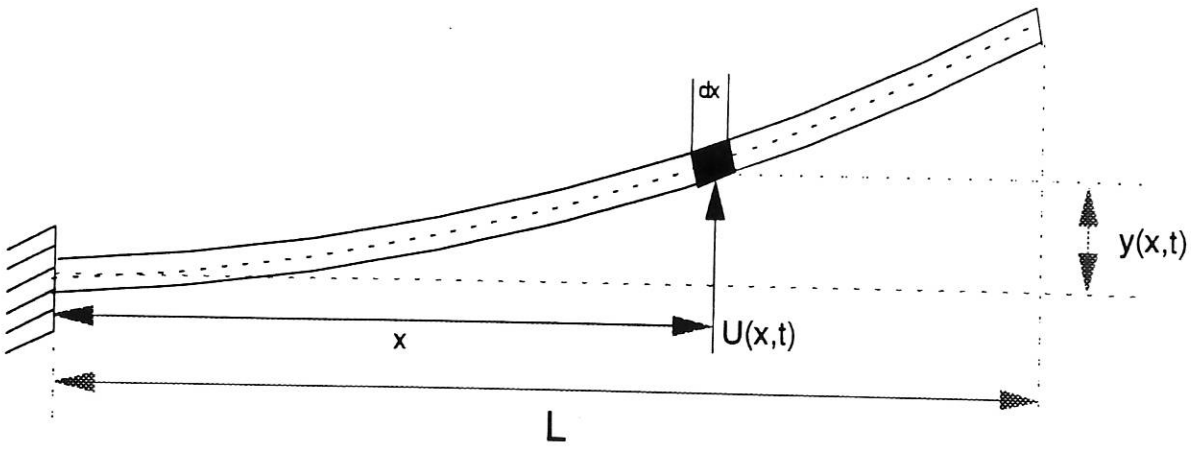

Figure 6: The cantilever beam in flexure.

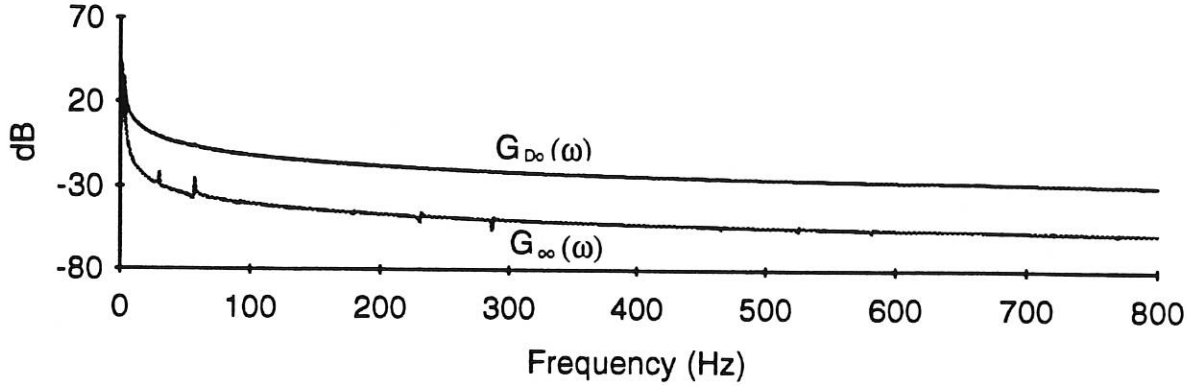

(a)

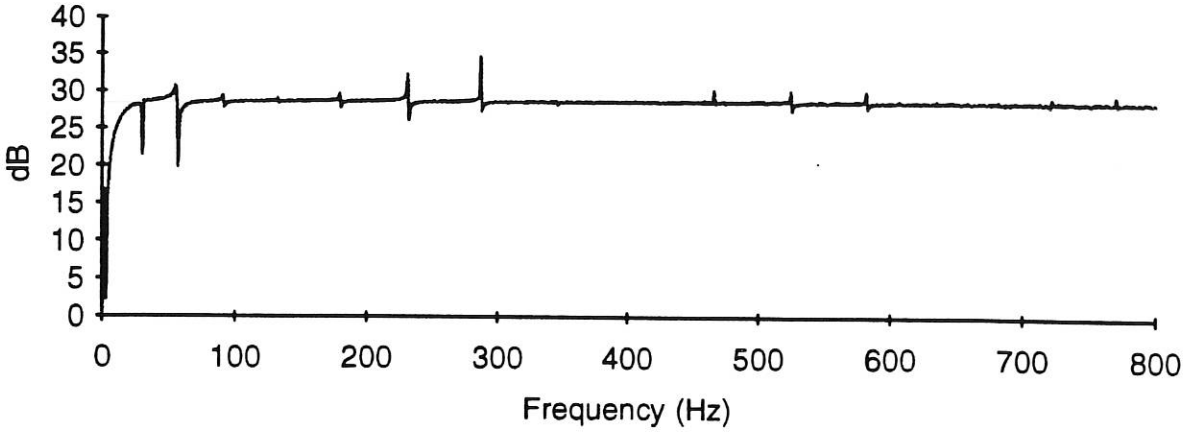

(b)

Figure 7: Performance of the self-tuning AVC system with fixed-free beam;
(a) Power densities before and after cancellation.
(b) Attenuation in spectral density.

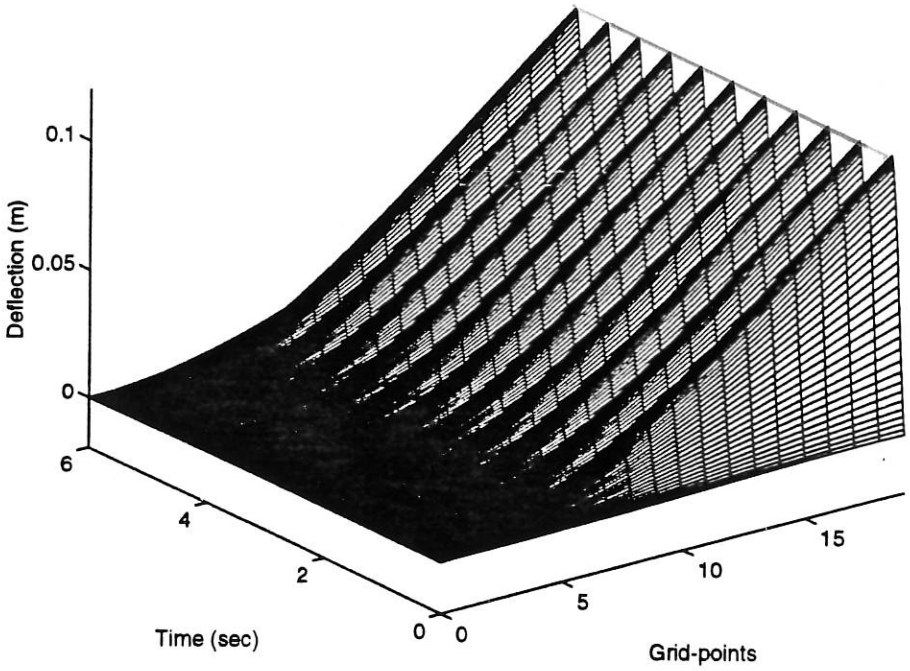

(a)

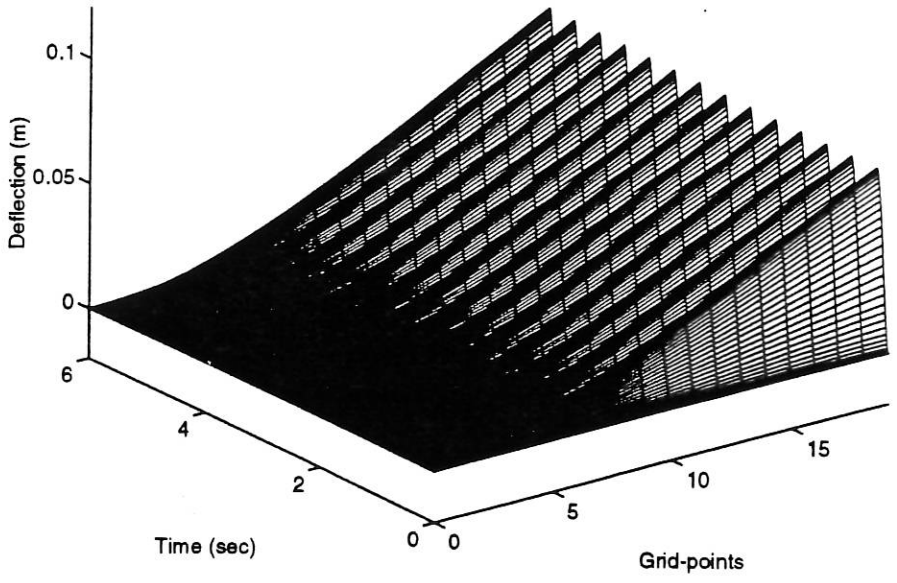

(b)

Figure 8: Performance of the self-tuning AVC system with fixed-free beam;
(a) Beam fluctuation before cancellation.
(b) Beam fluctuation after cancellation.

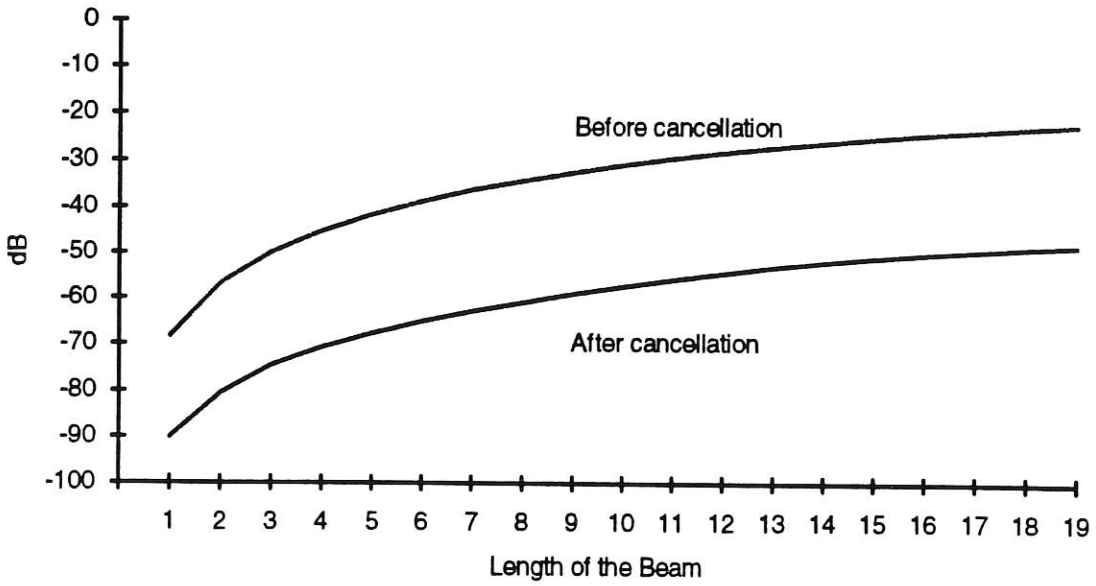

Figure 9: Average autopower spectral density level along (fixed-free) beam length.

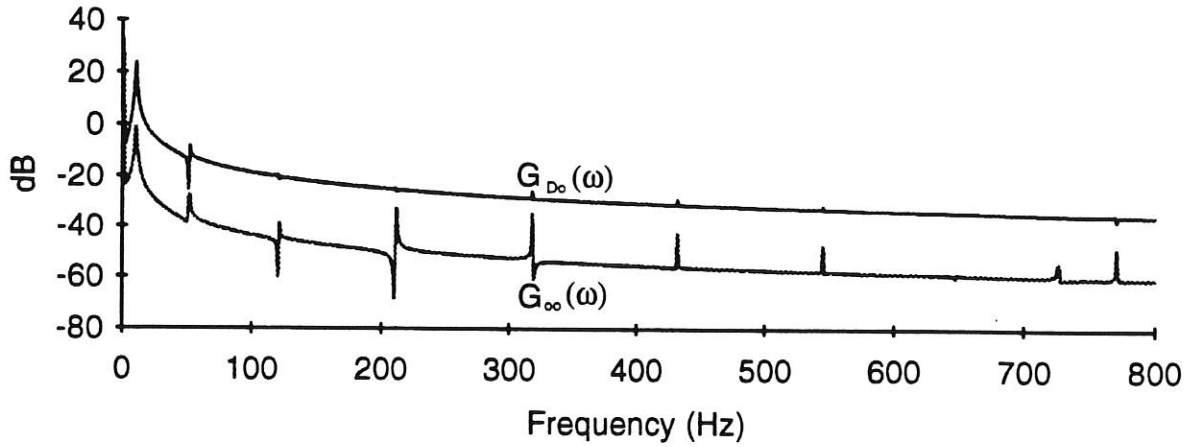

(a)

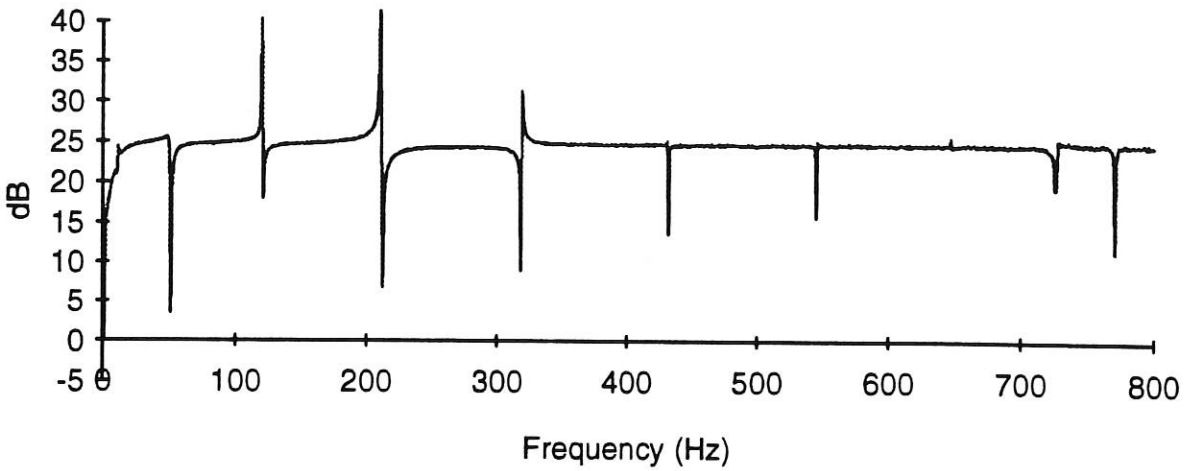

(b)

Figure 10: Performance of the self-tuning AVC system with the fixed-fixed beam;
(a) Power densities before and after cancellation.
(b) Cancelled spectrum.

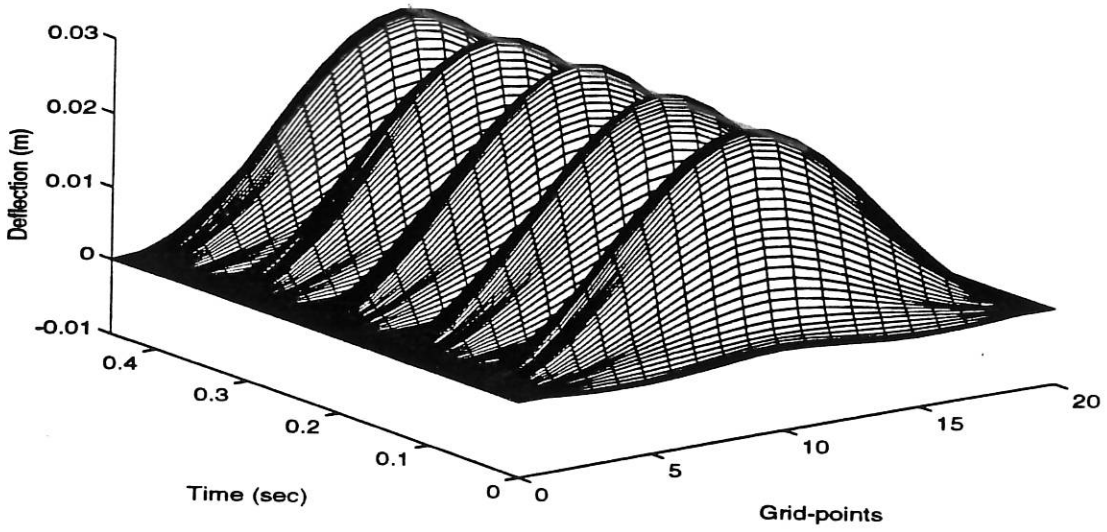

(a)

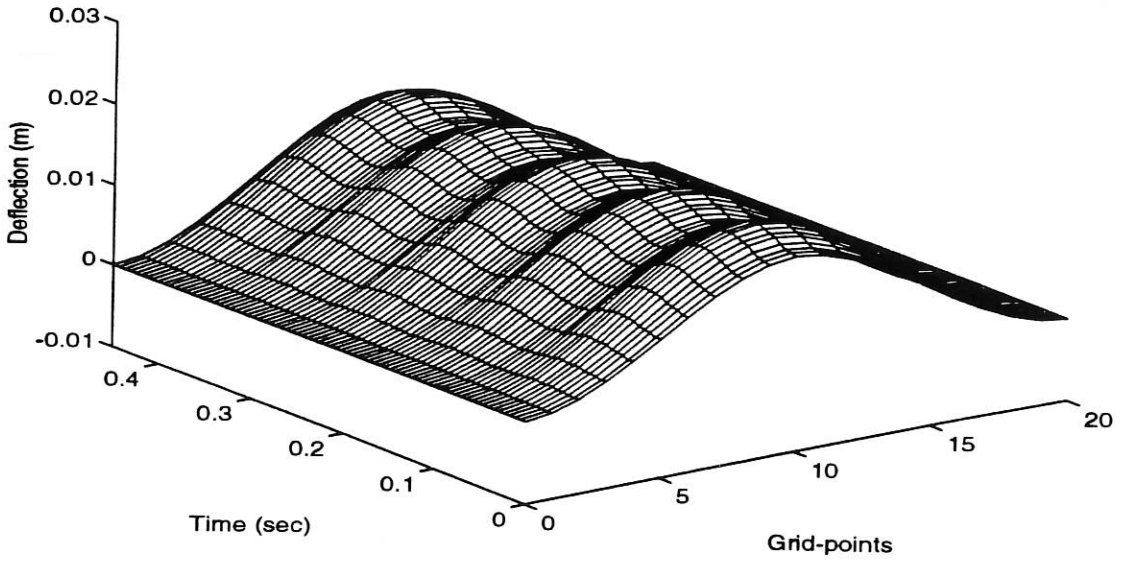

(b)

Figure 11: Performance of the self-tuning AVC system with the fixed-fixed beam;
(a) Beam fluctuation before cancellation.
(b) Beam fluctuation after cancellation.

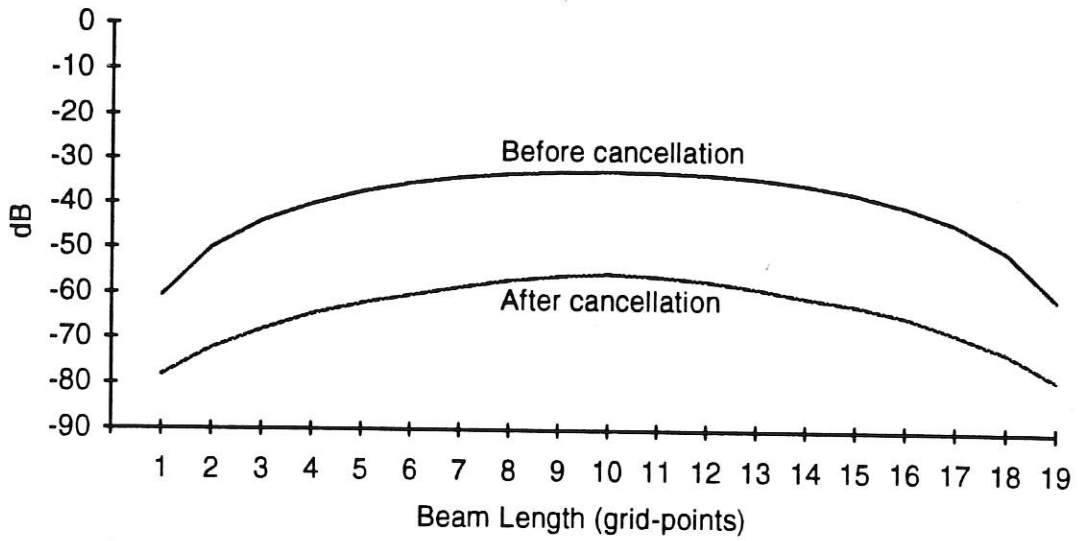

Figure 12: Average autopower spectral density level along the (fixed-fixed) beam length.